Inorg. Chem. **2003**, *42*, 3431–3437

Gallium and Indium Hydrazides. Molecular and Electronic Structure of $In[N(SiMe_3)NMe_2]_3$ and Related Compounds

Bing Luo, Christopher J. Cramer,* and Wayne L. Gladfelter*

Department of Chemistry and Supercomputer Institute, University of Minnesota, Minneapolis, Minnesota 55455

Received November 30, 2002

Gallium and indium hydrazides, $Ga[N(SiMe_3)NMe_2]_3$ (**1**) and $In[N(SiMe_3)NMe_2]_3$ (**2**), were synthesized from the reactions of metal chlorides and $Li[N(SiMe_3)NMe_2]$. Single crystal X-ray crystallographic analysis revealed that compound **2** was monomeric with trigonal planar geometries on the indium and the indium-bonded nitrogen atoms. The average In–N bond distance of 2.078(3) Å and the N–In–N–N dihedral angles did not provide clear structural evidence of In–N π-bonding. The electronic absorption spectra of the indium hydrazido complex revealed transitions at significantly lower energies compared to those observed in the tris(amido) compounds, $In[N(SiMe_3)_2]_3$ (**3**) and $In[N(^tBu)(SiMe_3)]_3$ (**4**). The absorptions of the indium and gallium compounds were attributed to ligand–metal charge transfer transitions. Trends in the electronic transitions for compounds **2** and **3** calculated at the time-dependent density functional and configuration interaction including single excitations levels, both using a minimal basis set, were consistent with the experimental data, and Mulliken charge analyses support the assignment to ligand-to-metal charge transfer transitions. These calculations also demonstrated the presence of π-bonding between the In and N p-orbitals, and an analogy is drawn to the frontier molecular orbitals of trimethylenemethane. The low-lying spectroscopic transition in **2**, and thus its yellow color, results from mixing of the lone pair electrons on the β-nitrogens of the hydrazido ligands with the HOMO of the InN_3 core.

Introduction

Group 13 metal nitrides and their composites are direct band gap semiconductors used in fabricating high-power, high-efficiency optoelectronic devices.[1] Practically, films of GaN and InN are prepared from tri(organyl) gallium or indium and ammonia in chemical vapor deposition processes.[1] In order to overcome the disadvantages of these conventional methods such as high temperatures and carbon contamination, new metal precursors and nitrogen sources have been extensively studied.[2] Hydrazine and its derivatives were investigated as alternative nitrogen sources to deposit GaN-containing films at lower temperatures.[3−6] Metal hydrazide derivatives are potential single-source precursors because of the presence of intramolecular metal−nitrogen bonds.[7]

Most of the group 13 metal hydrazide compounds studied to date feature ring or more complex cluster structures.[8−24]

* To whom correspondence should be addressed. E-mail: gladfelt@chem.umn.edu (W.L.G.) or cramer@chem.umn.edu.

(1) Stringfellow, G. B. *Organometallic Vapor-Phase Epitaxy*: *Theory and Practice*, 2nd ed.; Academic Press: New York, 1999.
(2) Neumayer, D. A.; Ekerdt, J. G. *Chem. Mater*. **1996**, *8*, 9−25.
(3) Gaskill, D. K.; Bottaka, N.; Lin, M. C. *J. Cryst. Growth* **1986**, *77*, 418−423.
(4) Lee, R. T.; Stringfellow, G. B. *J. Electron. Mater*. **1999**, *28*, 963−969.
(5) Friedman, D. J.; Norman, A. G.; Geisz, J. F.; Kurtz, S. R. *J. Cryst. Growth* **2000**, *208*, 11−17.
(6) Bourret-Courchesne, E.; Ye, Q.; Peters, D. W.; Arnold, J.; Ahmed, M.; Irvine, S. J. C.; Kanjolia, R.; Smith, L. M.; Rushworth, S. A. *J. Cryst. Growth* **2000**, *217*, 47−54.
(7) Lakhotia, V.; Neumayer, D. A.; Cowley, A. H.; Jones, R. A.; Ekerdt, J. G. *Chem. Mater*. **1995**, *7*, 546−552.
(8) Neumayer, D. A.; Cowley, A. H.; Decken, A.; Jones, R. A.; Lakhotia, W.; Ekerdt, J. G. *Inorg. Chem*. **1995**, *34*, 4698−4700.
(9) Wehmschulte, R. J.; Power, P. P. *Inorg. Chem*. **1996**, *35*, 2717−2718.
(10) Kim, Y.; Kim, J. H.; Park, J. E.; Song H.; Park, J. T. *J. Organomet. Chem*. **1997**, *545*−*546*, 99−103.
(11) Nöth, H.; Seifert, T. *Eur. J. Inorg. Chem*. **1998**, 1931−1938.
(12) Peters, D. W.; Power, M. P.; Bourret, E. D.; Arnold, J. *J. Chem. Soc., Chem. Commun*. **1998**, 753−754.
(13) Cho, D.; Park, J. E.; Bae, B.-J.; Lee, K.; Kim, B.; Park, J. T. *J. Organomet. Chem*. **1999**, *592*, 162−167.
(14) Gibson, V. C.; Redshaw, C.; White, A. J. P.; Williams, D. J. *Angew. Chem*. **1999**, *111*, 1014; *Angew. Chem., Int. Ed*. **1999**, *38*, 961−964.
(15) Uhl, W.; Molter, J.; Saak, W. *Z. Anorg. Allg. Chem*. **1999**, *625*, 321−328.
(16) Uhl, W.; Molter, J.; Koch, R. *Eur. J. Inorg. Chem*. **1999**, 2021−2027.
(17) Peters, D. W.; Bourret, E. D.; Power, M. P.; Arnold, J. *J. Organomet. Chem*. **1999**, *582*, 108−115.

10.1021/ic020693f CCC: $25.00
Published on Web 05/03/2003

In this study, we intended to use bulkier hydrazido ligands to prepare monomeric compounds that may have increased vapor pressures over the associated compounds. In addition, the targeted tris(hydrazido) compounds do not contain a direct metal−carbon bond, which could decrease carbon contamination if these are used as precursors. In this paper, we report the synthesis and characterization of the first examples of group 13 metal tris(hydrazido) derivatives, Ga[$N(SiMe_3)NMe_2]_3$ (**1**) and In[$N(SiMe_3)NMe_2]_3$ (**2**), and the unusual long-wavelength electronic absorptions for compound **2** and related amido indium compounds. Electronic structure calculations at the time-dependent density functional (TD-DFT) and configuration interaction including single excitations (CIS) levels of theory using a minimal basis set were carried out to understand the bonding and to aid in the spectroscopic analysis.

Experimental Section

Materials and General Procedures. Indium chloride and gallium chloride were purchased from Strem and used as received. All the other chemicals were obtained from Aldrich. The solutions of *n*-butyllithium in hexanes (2.5 M) and methyllithium in ether (1.4 M) were used as received. 1,1-Dimethylhydrazine and chlorotrimethylsilane were distilled over calcium hydride under nitrogen. In[$N(SiMe_3)_2]_3$[25,26] (**3**) and In[$N(SiMe_3)(^tBu)]_3$[27] (**4**) were prepared according to the literature methods. Diethyl ether and hexanes were predried over calcium hydride and freshly distilled over sodium/benzophenone under nitrogen. The spectrophotometric-grade hexanes used in the absorption spectroscopic experiments were distilled over calcium hydride under nitrogen and were degassed by the repeating freeze/pump/thaw process. Benzene-d_6 was distilled over calcium hydride under nitrogen. All experiments were conducted under an oxygen-free, dry-nitrogen atmosphere using Schlenk and glovebox techniques.

^{1}H NMR spectra were obtained in benzene-d_6 solutions at room temperature on a Varian INOVA 300 spectrometer, and the residual proton (δ 7.15) in C_6D_6 was used as the internal standard. The IR spectra of KBr pellets for solids and liquid films within NaCl windows for liquids were recorded on a Nicolet MAGNA-IR 560 spectrometer. Chemical-ionization mass spectra were acquired on a Finnigan Mat 95 spectrometer using a direct insertion probe. The samples were evaporated at the temperature range 25−340 °C, and the ionization gas mixture was methane with 4% ammonia. The electronic absorption spectra were recorded in a modified Varian Cary spectrometer. Melting points were measured in sealed glass capillaries and were uncorrected. The elemental analyses were performed by Schwarzkopf Microanalytical Laboratory, Woodside, NY, and Desert Analytics, Tucson, AZ.

Synthesis of $HN(SiMe_3)NMe_2$. To a stirred solution of H_2NNMe_2 (11.9 g, 197 mmol) in 20 mL of Et_2O at −78 °C was added an ether solution of methyllithium (135 mL, 197 mmol). After the mixture was allowed to warm to room temperature and stirred for 4 h, it was again cooled at −78 °C, and Me_3SiCl (25.1 mL, 197 mmol) was added. A white precipitate formed immediately, and the mixture was allowed to warm to room temperature, stirred for 14 h, and filtered to separate a white solid (LiCl) and a colorless filtrate. Ether was distilled off from the filtrate at low temperatures, and a colorless liquid (14 g, 54% yield) was collected in the temperature range 75−80 °C under a reduced nitrogen pressure (ca. 100 Torr). ^{1}H NMR: δ 0.13 (9H, s, $SiCH_3$), 1.72 (1H, br s, NH), 2.21 (6H, s, NCH_3). IR (cm^{-1}): 3284 (ν_{NH}, w), 2986 s, 2949 s, 2896 m, 2849 m, 2811 s, 2764 s, 1464 m, 1450 m, 1434m, 1400 w, 1376 w, 1297 w, 1259 s, 1247 s, 1220 w, 1153 w, 1091 m, 1063 s, 1010 m, 968 w, 897 s, 837 s, 803 m, 747 w, 720 w, 684 w.

Synthesis of Ga[$N(SiMe_3)NMe_2]_3$ (1). To a stirred solution of $HN(SiMe_3)NMe_2$ (1.75 g, 13.2 mmol) in 20 mL of hexanes at −78 °C was added a hexanes solution of *n*-BuLi (5.28 mL, 13.2 mmol). The mixture was heated at 70 °C for 1 h, and a colorless solution was obtained. After the solution was cooled to room temperature, it was added to a solution of $GaCl_3$ (0.774 g, 4.40 mmol) in 20 mL of Et_2O at −78 °C. The mixture was allowed to warm to room temperature, and a white precipitate formed during the warming process. The slurry was stirred for 18 h, and a filtration was carried out to separate the white precipitate (LiCl) and a colorless filtrate. After the filtrate was concentrated to ca. 5 mL and stored at −50 °C, colorless plates were collected (1.32 g, 65% yield). The sample used in collecting the absorption spectrum was recrystallized twice from spectrophotometric-grade hexanes. Mp: 75.0−78.0 °C. ^{1}H NMR: δ 0.30 (27H, s, $SiCH_3$), 2.64 (18H, s, NCH_3). IR (cm^{-1}): 2975 s, 2944 s, 2892 s, 2858 s, 2826 m, 2801 s, 2776 m, 2744 s, 2655 w, 1465 s, 1447 s, 1435 s, 1420 m, 1409 w, 1395 m, 1353 w, 1303 m, 1246 s, 1220 s, 1157 w, 1087 m, 1021 s, 1010 s, 945 s, 924 s, 833 s, 748 s, 739 s, 678 s. CI MS (assignment, % relative intensity): 463 [$(M + H)^+$, 14.4], 447 [$(M - Me)^+$, 28.7}, 348 [{$M - N(SiMe_3)NMe_2 + NH_3\}^+$, 19.9}, 331 [{$M - N(SiMe_3)NMe_2\}^+$, 100}, 133 [{$H_2N(SiMe_3)NMe_2\}^+$, 11.0}. Anal. Calcd for $C_{15}H_{45}N_6Si_3Ga$: C, 38.87; H, 9.78; N, 18.13. Found: C, 37.68; H, 10.07; N, 17.64.

Synthesis of In[$N(SiMe_3)NMe_2]_3$ (2). To a stirred solution of $HN(SiMe_3)NMe_2$ (2.69 g, 20.3 mmol) in 20 mL of hexanes at −78 °C was added a hexanes solution of *n*-BuLi (8.14 mL, 20.3 mmol). The mixture was heated at 70 °C for 1 h, and a colorless solution was obtained. After the solution was cooled to room temperature, it was added into a slurry of $InCl_3$ (1.50 g, 6.78 mmol) in 20 mL of Et_2O at −78 °C. The mixture was allowed to warm to room temperature and stirred for 18 h. A filtration was carried out to yield a white precipitate (LiCl) and a yellow filtrate. After the filtrate was concentrated to ca. 10 mL and stored at −20 °C overnight, yellow blocks were collected (2.42 g, 70% yield). The sample used in collecting the absorption spectrum was recrystallized twice from spectrophotometric-grade hexanes. Mp: 75 °C, decomp without melting. ^{1}H NMR: δ 0.29 (27H, s, $SiCH_3$), 2.68 (18H, s, NCH_3). IR (cm^{-1}): 2981 m, 2944 m, 2892 m, 2837 m, 2816 w, 2791 m, 2763 m, 2706 m, 2651w, 1458 s, 1442 s, 1418 s, 1394 m, 1351 w, 1296 w, 1246 s, 1238 s, 1221 s, 1152 s, 1086 w, 1041 s, 1030 s, 1008 s, 908 s, 826 s, 745 s, 733 s, 677 s. CI MS (assignment, % relative intensity): 508 [M^+, 0.3], 377 [{$M - N(SiMe_3)NMe_2\}^+$, 1.5], 362 [{$M - N(SiMe_3)NMe_2 - Me\}^+$, 2.6], 245 [a species

(18) Silverman, J. S.; Abernethy, C. D.; Jones, R. A.; Cowley, A. H. *J. Chem. Soc., Chem. Commun.* **1999**, 1645−1646.
(19) Luo, B.; Gladfelter, W. L. *J. Chem. Soc., Chem. Commun.* **2000**, 825−826.
(20) Uhl, W.; Molter, J.; Neumüller, B. *Organometallics* **2000**, *19*, 4422−4424.
(21) Uhl, W.; Molter, J.; Koch, R. *Eur. J. Inorg. Chem.* **2000**, 2255−2262.
(22) Uhl, W.; Molter, J.; Neumüller, B.; Saak, W. *Z. Anorg. Allg. Chem.* **2000**, *626*, 2284.
(23) Uhl, W.; Molter, J.; Neumüller, B. *Inorg. Chem.* **2001**, *40*, 2011−2014.
(24) Nöth, H.; Seifert, T. *Eur. J. Inorg. Chem.* **2002**, 602−612.
(25) Bürger, H.; Cichon, J.; Goetze, U.; Wannagat, U.; Wismar, H. J. *J. Organomet. Chem.* **1971**, *33*, 1−12.
(26) Pretrie, M. A.; Ruhlandt-Senge, K.; Hope, H.; Power, P. P. *Bull. Soc. Chim. Fr.* **1993**, *130*, 851.
(27) Kim, J.; Bott, S. G.; Hoffman, D. M. *Inorg. Chem.* **1998**, *37*, 3835−3841.

Table 1. Crystallographic Data for Compound **2**

chemical formula	$C_{15}H_{45}InN_6Si_3$
fw	508.66
space group	$P\bar{1}$
a, Å	14.426(1)
b, Å	14.546(1)
c, Å	14.695(1)
α, deg	73.644(1)
β, deg	72.307(1)
γ, deg	73.312(1)
V, Å^3	2749.6(4)
Z	4
T (°C)	−100
λ, Å	0.71073
(*ρ* calcd, g cm^{-3})	1.229
μ, cm^{-1}	10.01
R1, wR2[a] [$I > 2\sigma(I)$]	0.0234, 0.0559

[a] $R1 = \sum||F_o| - |F_c||/\sum|F_o|$ and $wR2 = \{\sum[w(F_o^2 - F_c^2)^2]/\sum[w(F_o^2)^2]\}^{1/2}$, where $w = 1/[\sigma^2(F_o^2) + (aP)^2 + (bP)]$, $P = (F_o^2 + 2F_c^2)/3$, and *a* and *b* are constants given in Supporting Information.

containing an indium and a silicon, 46.1], 133 [$\{H_2N(SiMe_3)NMe_2\}^+$, 100]. Anal. Calcd for $C_{15}H_{45}N_6Si_3In$: C, 35.42; H, 8.92; N, 16.52. Found: C, 35.13; H, 9.07; N, 16.48.

Electronic Absorption Spectra. The spectroscopic-grade hexanes solutions of compounds **1** (0.06 mM), **2** (0.08 mM), **3** (0.13 mM), and **4** (0.15 mM) were sealed in quartz cells (1 cm) under nitrogen. All spectra were recorded in the wavelength range 190−600 nm and were corrected with background subtractions.

X-ray Data Collection, Structure Solution, and Refinement. A crystal of compound **2** was mounted on a glass fiber under a nitrogen atmosphere. The data collection was conducted on a Siemens SMART system. An initial set of cell constants was calculated from reflections harvested from three sets of 30 frames. These sets of frames were oriented such that orthogonal wedges of reciprocal space were surveyed. The data collection technique was generally known as a hemisphere collection. A randomly oriented region of reciprocal space was surveyed to the extent of 1.3 hemispheres to a resolution of 0.77 Å. Three major swaths of frames were collected with 0.30° steps in *ω*. Because the lattice was triclinic, 50 additional sets of frames were collected to better model the absorption correction. The final cell constants were calculated from a set of 8192 strong reflections.

The space group $P\bar{1}$ was determined on the basis of the lack of systematic absences and on the basis of intensity statistics. A successful direct-methods solution was applied to the structure that provided most non-hydrogen atoms from the *E*-map. Several full-matrix, least-squares/difference Fourier cycles were performed which located the remainder of the non-hydrogen atoms. All non-hydrogen atoms were refined with anisotropic displacement parameters. All hydrogen atoms were placed in ideal positions and refined as riding atoms with relative isotropic displacement parameters. The experimental conditions and unit cell information are summarized in Table 1.

Calculations. The geometries employed for compounds **2** and **3** were those from single crystal XRD structures. Because of the structural similarity of the two molecules in the asymmetric unit in the structure of **2**, the set of coordinates for the molecule containing In(1) was used. The electronic transitions for compounds **2** and **3** were calculated at the TD-DFT[28a] and CIS[28b] levels of theory using the STO-3G basis set. This requires 204 and 240 basis functions for compounds **2** and **3**, respectively. The TD-DFT calculations are expected to be more accurate for the prediction of absorption wavelengths (although the use of a minimal basis set suggests that only qualitative results should be expected),[28c] while the CIS calculations are useful because they provide wave functions for the excited states that can be analyzed for other properties, like partial atomic charges. Computed excitation energies from the CIS level were inferior to those from the TDDFT calculations and, indeed, were very inaccurate in some instances. The generally poorer performance of CIS compared to TD-DFT has been amply documented in the literature.[28c−e] The DFT functional employed for the TD-DFT calculations was the PBE1PBE functional of Perdew, Burke, and Enzerhof.[28f] Choice of the PBE1PBE functional was motivated by its generally robust performance for excited-state calculations.[28d,g] All calculations used the Gaussian 98 program package.[28h]

Results

Synthesis and Characterization of Ga[N(SiMe$_3$)NMe$_2$]$_3$ (1) and In[N(SiMe$_3$)NMe$_2$]$_3$ (2). Compounds **1** (65% yield) and **2** (70% yield) were prepared as colorless and yellow crystals, respectively, from the reactions summarized in eqs 1 and 2 and were characterized by elemental analysis and spectroscopic methods. The reactant $HN(SiMe_3)NMe_2$ was prepared as a colorless liquid from the reaction of Me_3SiCl with $LiNHNMe_2$ generated in situ from the lithiation of H_2NNMe_2.

$$3HN(SiMe_3)NMe_2 + 3n\text{-BuLi} \xrightarrow[-78 \text{ to } 70\ ^\circ\text{C, } 1\text{ h}]{\text{hexanes}} 3Li[N(SiMe_3)NMe_2] + 3n\text{-Bu-H} \quad (1)$$

$$3Li[N(SiMe_3)NMe_2] + MCl_3 \xrightarrow[25\ ^\circ\text{C, } 18\text{ h}]{Et_2O} M[N(SiMe_3)NMe_2]_3 + 3LiCl \quad (2)$$

M = Ga (**1**) and In (**2**)

The ^{1}H NMR spectra exhibited singlets of the $SiMe_3$ and NMe_2 groups at 0.30 and 2.64 ppm, respectively, for **1** and 0.29 and 2.68 ppm, respectively, for **2**. In the chemical-ionization spectrum of **1**, the parent ion (plus 1) was found to be 14% of the base peak $[M - N(SiMe_3)NMe_2]^+$. For **2**, the base peak was attributed to $[H_2NSiMe_3NMe_2]^+$. The peaks centered at 245 with the intensity of 46% of the base peak could not be specifically assigned, but the isotope distribution of the peaks showed that they belonged to a species containing an indium and a silicon atom. The intensities of all other peaks including the parent ion peak

(28) (a) Koch, W.; Holthausen, M. C. *A Chemist's Guide to Density Functional Theory*; Wiley-VCH: Weinheim, 2000. (b) Foresman, J. B.; Head-Gordon, M.; Pople, J. A.; Frisch, M. J. *J. Phys. Chem.* **1992**, *96*, 135. (c) Bauernschmitt, R.; Ahlrichs, R. *Chem. Phys. Lett.* **1996**, *256*, 454. (d) Cramer, C. J. *Essentials of Computational Chemistry*; Wiley: Chichester, 2002; pp 441−469. (e) Stratmann, R. E.: Scuseria, G. E.; Frisch, M. J. *J. Chem. Phys.* **1998**, *109*, 8218. (f) Burke, K.; Ernzerhof, M.; Perdew, J. P. *Chem. Phys. Lett.* **1997**, *265*, 115. (g) Adamo, C.; Barone, V. *Chem. Phys. Lett.* **1999**, *314*, 152. (h) Frisch, M. J.; Trucks, G. W.; Schlegel, H. B.; Scuseria, G. E.; Robb, M. A.; Cheeseman, J. R.; Zakrzewski, V. G.; Montgomery, J. A., Jr.; Stratmann, R. E.; Burant, J. C.; Dapprich, S.; Millam, J. M.; Daniels, A. D.; Kudin, K. N.; Strain, M. C.; Farkas, O.; Tomasi, J.; Barone, V.; Cossi, M.; Cammi, R.; Mennucci, B.; Pomelli, C.; Adamo, C.; Clifford, S.; Ochterski, J.; Petersson, G. A.; Ayala, P. Y.; Cui, Q.; Morokuma, K.; Malick, D. K.; Rabuck, A. D.; Raghavachari, K.; Foresman, J. B.; Cioslowski, J.; Ortiz, J. V.; Stefanov, B. B.; Liu, G.; Liashenko, A.; Piskorz, P.; Komaromi, I.; Gomperts, R.; Martin, R. L.; Fox, D. J.; Keith, T.; Al-Laham, M. A.; Peng, C. Y.; Nanayakkara, A.; Gonzalez, C.; Challacombe, M.; Gill, P. M. W.; Johnson, B. G.; Chen, W.; Wong, M. W.; Andres, J. L.; Head-Gordon, M.; Replogle, E. S.; Pople, J. A. *Gaussian 98*; Gaussian, Inc.: Pittsburgh, PA, 1998.

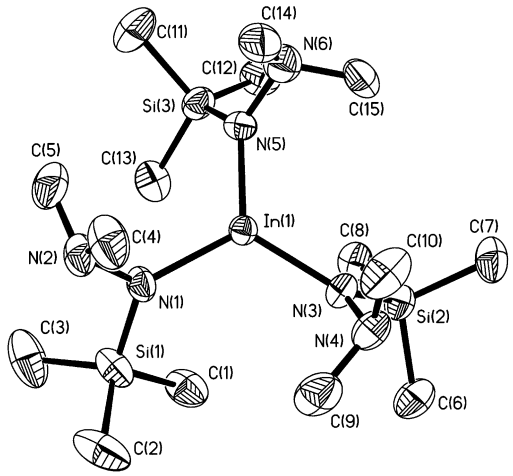

Figure 1. Structure and atom labeling scheme for one molecule in the asymmetric unit of the structure of $In[N(SiMe_3)NMe_2]_3$ (**2**). Atoms are shown at the 50% probability level. All hydrogen atoms are omitted for clarity.

Table 2. Selected Bond Lengths (Å) and Angles (deg) for $In[N(SiMe_3)NMe_2]_3$ (**2**)

In(1)−N(1)	2.0752(16)	N(1)−N(2)	1.443(2)
In(1)−N(3)	2.0802(16)	N(3)−N(4)	1.440(2)
In(1)−N(5)	2.0768(16)	N(5)−N(6)	1.445(2)
In(2)−N(7)	2.0753(15)	N(7)−N(8)	1.445(2)
In(2)−N(9)	2.0796(16)	N(9)−N(10)	1.440(2)
In(2)−N(11)	2.0812(15)	N(11)−N(12)	1.443(2)
N(1)−Si(1)	1.7199(17)	N(7)−Si(4)	1.7243(16)
N(3)−Si(2)	1.7252(17)	N(9)−Si(5)	1.7248(16)
N(5)−Si(3)	1.7189(18)	N(11)−Si(6)	1.7200(16)
N(1)−In(1)−N(3)	118.88(7)	In(1)−N(5)−N(6)	122.56(13)
N(1)−In(1)−N(5)	118.15(7)	In(1)−N(5)−Si(3)	126.93(9)
N(3)−In(1)−N(5)	122.47(7)	N(6)−N(5)−Si(3)	110.33(12)
N(7)−In(2)−N(9)	121.08(6)	In(2)−N(7)−N(8)	122.55(11)
N(7)−In(2)−N(11)	118.40(6)	In(2)−N(7)−Si(4)	126.99(9)
N(9)−In(2)−N(11)	120.18(6)	N(8)−N(7)−Si(4)	110.42(11)
In(1)−N(1)−N(2)	122.87(12)	In(2)−N(9)−N(10)	122.21(11)
In(1)−N(1)−Si(1)	126.74(9)	In(2)−N(9)−Si(5)	128.15(9)
N(2)−N(1)−Si(1)	110.32(12)	N(10)−N(9)−Si(5)	109.63(12)
In(1)−N(3)−N(4)	122.33(12)	In(2)−N(11)−N(12)	122.20(11)
In(1)−N(3)−Si(2)	127.58(9)	In(2)−N(11)−Si(6)	127.01(8)
N(4)−N(3)−Si(2)	110.08(12)	N(12)−N(11)−Si(6)	110.69(11)

at 508 (0.3%) were below 3%. The elemental analysis results were satisfactory except that the measured carbon percentage of compound **1** was 1.2% lower than the calculated values.

Structure of $In[N(SiMe_3)NMe_2]_3$ (2). Compound **2** crystallized in the space group of $P\bar{1}$ with two chemically identical, monomeric molecules in the asymmetric unit. The molecular structure of one molecule is shown in Figure 1. The structural parameters of the two molecules were similar, and the selected bond lengths and angles are given in Table 2.

In both molecules, the indium atoms were three-coordinate adopting a trigonal planar geometry. The bond angles at indium varied from 118.15(7)° to 122.47(7)°, and the In−N bond lengths from 2.0752(16) to 2.0812(15) Å. These In−N bond lengths were comparable to those in other three-coordinate indium complexes including $In[N(SiMe_3)_2]_3$ [2.049(1) Å],[26] $^tBu_2In[N(SiPh_3)(2,6\text{-}^iPr_2C_6H_3)]$ [2.104(3) Å],[26] In(2,2,6,6-tetramethylpiperidino)$_3$ [2.068(5) and 2.087(5) Å],[29] $(2,4,6\text{-}^tBu_3C_6H_2)In[N(SiMe_3)_2]_2$ [2.094(4) and 2.103(6) Å],[30] and $In[N(H)(2,4,6\text{-}^tBu_3C_6H_2)]_3$ [2.061(7)−2.075(6) Å].[31] It is noteworthy that these In−N bond lengths are also similar to some four-coordinate tris(amido) indium compounds such as $In[NPh(SiMe_3)]_3(OEt_2)$ [2.083(2)−2.103(2) Å][27] and $In(NPh_2)_3(py)$ [2.072(3)−2.099(3) Å].[27] The geometries of the α-nitrogens (those bonded to indium) were trigonal planar, and those of the β-nitrogens were trigonal pyramidal. Angles between the coordination plane on the indiums and the α-nitrogens were in the ranges 52−57.8° and 51.5−59.9° for the two molecules in the asymmetric unit.

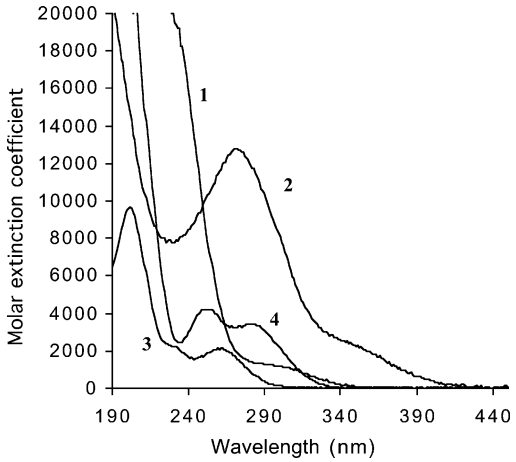

Figure 2. Electronic absorption spectra of $Ga[N(SiMe_3)NMe_2]_3$ (**1**), $In[N(SiMe_3)NMe_2]_3$ (**2**), $In[N(SiMe_3)_2]_3$ (**3**), and $In[N(SiMe_3)CMe_3]_3$ (**4**).

Electronic Absorption Spectra of Compounds 1−4. All four of these compounds exhibited more or less distinct absorptions in the ultraviolet spectral region. The electronic absorption spectra of compounds **1**−**4** are displayed in Figure 2, and Table 4 lists the specific values for λ_{max} and the molar extinction coefficients. Detailed assignments of the transitions leading to these spectral features are discussed in the following section. At room temperature, solutions of these compounds did not exhibit detectable emission.

Discussion

The significance of π-interactions between metal and nitrogen in heavy group 13 metal amides has been the topic of several studies.[32−36] Power and co-workers concluded that these interactions, if they exist, are insignificant.[36] The structure determination of **2** supports this statement at least insofar as geometry is concerned. As described already, the In−N bond lengths in the structures of **2** and other amido

(29) Frey, R.; Gupta, V. D.; Linti, G. *Z. Anorg. Allg. Chem.* **1996**, *622*, 1060.
(30) Leung W.-P.; Chan, C. M. Y.; Wu, B.-M.; Mak, T. C. W. *Organometallics* **1996**, *15*, 5179−5184.
(31) Silverman, J. S.; Carmalt, C. J.; Cowley, A. H.; Culp, R. D.; Jones, R. A.; McBurnett, B. G. *Inorg. Chem.* **1999**, *38*, 296−300.
(32) Waggoner, K.; Power, P. P. *J. Am. Chem. Soc.* **1991**, *113*, 3385−3393.
(33) Waggoner, K. M.; Ruhlandt-Senge, K.; Wehmschulte, R. J.; He, M.; Olmstead, M. M.; Power. P. P. *Inorg. Chem.* **1993**, *32*, 2557−2561.
(34) Brothers, P. J.; Wehmschulte, R. J.; Olmstead, M. M.; Ruhlandt-Senge, K.; Parkin, S. R.; Power, P. P. *Organometallics* **1994**, *13*, 2792−2799.
(35) Atwood, D. A.; Atwood, V. O.; Cowley, A. H.; Jones, R. A.; Atwood, J. L.; Bott, S. G. *Inorg. Chem.* **1994**, *33*, 3251−3254.
(36) Brothers, P. J.; Power, P. P. *Adv. Organomet. Chem.* **1996**, *39*, 1−69.

Table 3. Important Angles (deg) between the Coordination Planes on the Indiums and α-Nitrogens for the Structure of **2**[a]

plane 1	plane 2	angle (deg)
	Molecule 1	
In(1)N(1)N(3)N(5) (0.0320 Å)	**N(1)**In(1)N(2)Si(1)	52.0
In(1)N(1)N(3)N(5)	**N(3)**In(1)N(4)Si(2)	55.9
In(1)N(1)N(3)N(5)	**N(5)**In(1)N(6)Si(3) (0.0158 Å)	57.8
N(1) In(1)N(2)Si(1) (0.0098 Å)	**N(3)**In(1)N(4)Si(2)	88.1
N(1) In(1)N(2)Si(1)	**N(5)**In(1)N(6)Si(3)	90.4
N(3) In(1)N(4)Si(2) (0.0042 Å)	**N(5)**In(1)N(6)Si(3)	93.5
	Molecule 2	
In(2)N(7)N(9)N(11) (0.0265 Å)	**N(7)**In(2)N(8)Si(4)	51.5
In(2)N(7)N(9)N(11)	**N(9)**In(2)N(10)Si(5)	56.1
In(2)N(7)N(9)N(11)	**N(11)**In(2)N(12)Si(6) (0.0115 Å)	59.9
N(7) In(2)N(8)Si(4) (0.0079 Å)	**N(9)**In(2)N(10)Si(5)	89.9
N(7) In(2)N(8)Si(4)	**N(11)**In(2)N(12)Si(6)	90.5
N(9) In(2)N(10)Si(5) (0.0012 Å)	**N(11)**In(2)N(12)Si(6)	94.3

[a] Each plane was represented by four atoms with the first atom in bold being the center atom. The distances in parentheses were the mean derivations of the four atoms from the planes. The torsion angles are the angles between the normals of the planes.

Table 4. Observed Electronic Transitions for Compounds **1**−**4**

compd	obsd λ, nm (ϵ, M^{-1} cm^{-1})	calcd λ, nm	oscillator strength	assignment[b]
1	295 (1200)			
2	350 (2200)	362	0.03	HOMO → LUMO
		357	0.03	HOMO − 1 → LUMO
	271 (13000)	276	0.03	HOMO − 3 → LUMO
		274	0.02	HOMO − 4 → LUMO
3	259 (2200)	262	0.07	HOMO → LUMO
		262	0.07	HOMO − 1 → LUMO
	230 (2200)	229	0.06	HOMO → LUMO+1
		229	0.06	HOMO − 1 → LUMO + 1
	202 (10000)	203	0.01	HOMO − 2 → LUMO + 1
4	281 (3300)			HOMO → LUMO
				HOMO − 1 → LUMO
	253 (4100)			HOMO → LUMO + 1
				HOMO − 1 → LUMO + 1

[a] Calculated electronic transitions at the TD-DFT/STO-3G are presented for compounds **2** and **3**. [b] The HOMO and HOMO − 1 levels in both **2** and **3** and the HOMO − 3 and HOMO − 4 levels in **2** are very nearly degenerate.

compounds containing a three-coordinate indium are comparable to four-coordinate indium compounds. The large angles (51.5−59.9°, see Table 3) between the coordination plane of the indium and those of the α-nitrogens must significantly decrease the π-interaction between the sp^2-hybridized indium and nitrogen atoms owing to reduced p−p overlap.

Amido indium compounds having a yellow or brown color were previously observed for $In(NPh_2)_3(py)$,[27] $In[NMe(SiMe_3)]_3(p\text{-}Me_2Npy)$,[27] $In[N(H)(2,4,6\text{-}{}^tBu_3C_6H_2)]_3$,[31] and $In[N(H)(2,6\text{-}{}^iPr_2C_6H_3)](py)_2$.[31] No assignment of the absorption peaks in any of these molecules has previously been attempted. To address this situation, we carried out electronic structure calculations to better characterize the lower energy electronic transitions. Because of the large size of these molecules, calculations were only undertaken for compounds **2** and **3**, but a comparison of these two already reveals some interesting phenomena. TD-DFT/STO-3G calculations using the input coordinates obtained from the XRD structures provided the calculated transitions listed in Table 4. Although only a minimal basis set is employed, the trends in the absorption spectra predicted at this level of theory mimic those observed experimentally. In particular, both **2** and **3** have lowest-energy absorptions of moderate oscillator strength, with those of **2** at significantly lower energies than those of **3**.

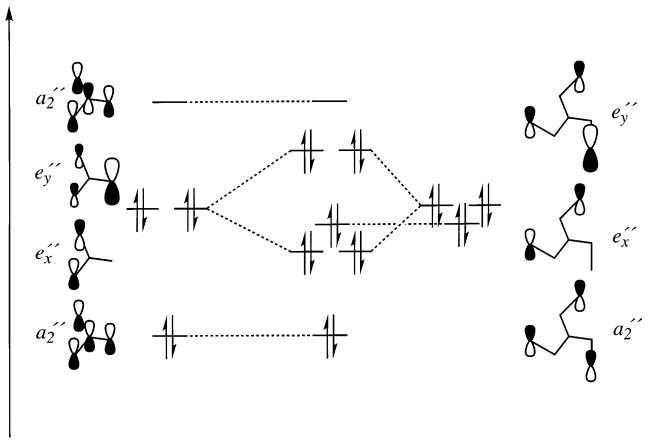

Figure 3. TMM-like π-orbitals (left, corresponding to **3**), β-nitrogen lone pair hybrid orbitals (right), and their mixing (center, corresponding to **2**).

There is a good correspondence in the overall character of several of the low-energy excitations in both **2** and **3**, even though the transition energies are significantly different. For instance, both show longest wavelength absorptions that are effectively 2-fold degenerate because the energies of the highest occupied molecular orbital (HOMO) and the next highest occupied MO (HOMO − 1) are very close to one another, and thus, single-electron excitations into the lowest unoccupied molecular orbital (LUMO) out of either occur at similar wavelengths. In addition, there is also a non-degenerate excitation from HOMO − 2 to LUMO in both **2** and **3** that occurs with effectively negligible oscillator strength. Finally, in each case there are effectively degenerate excitations from HOMO and HOMO − 1 to LUMO + 1 that occur with moderate oscillator strength (the HOMO − 1 to LUMO + 1 excitation for **2** does not appear in Table 4 but is predicted to be the seventh lowest-energy excitation). One feature that does differentiate **2** from **3**, beyond the lower energy required for the absorptions in **2** already discussed, is the presence of nearly degenerate absorptions from HOMO − 3 and HOMO − 4 into the LUMO with weak oscillator strength.

Inspection of the molecular orbitals involved indicates that these spectral features derive from distorted p−p π-interactions analogous to those found in the prototypical Y-shaped π-system, trimethylenemethane (TMM).[37,38] As illustrated in Figure 3 using symmetry labels consistent with the D_{3h} point group, the TMM π-system has a low-energy orbital belonging to the a_2'' irreducible representation (irrep) that has entirely in-phase overlap of the p-orbitals. This is followed by two degenerate nonbonding orbitals belonging to the e_x'' and e_y'' irreps, and finally, a fully antibonding orbital again

(37) Cramer, C. J.; Smith, B. A. *J. Phys. Chem.* **1996**, *100*, 9664.
(38) Li, J.; Worthington, S. E.; Cramer, C. J. *J. Chem. Soc., Perkin Trans. 2* **1998**, 1045.

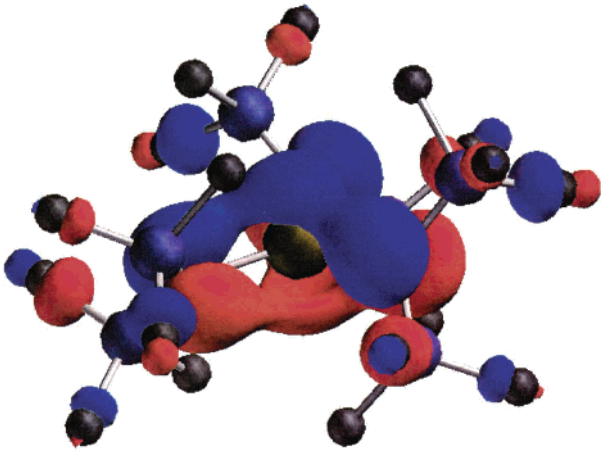

Figure 4. Fully bonding TMM-like π-orbital for **3** shown at the 0.03 au isocontour level; hydrogen atoms have been deleted for clarity.

belonging to the a_2'' irrep. In the case of an indium amide, the system has 6 π-electrons from the 3 nitrogen lone pairs, and one would thus expect the lowest energy electronic transition to be degenerate and dipole-allowed from either of the two nonbonding levels to the antibonding level. The next lowest energy single-electron excitation would be dipole forbidden from the fully bonding level to the fully antibonding level.

Although it is somewhat surprising that this situation applies, insofar as there is obviously a large "twisting" of the In−N π-bonds, visualization of the MOs reveals the TMM analysis to be valid. Figure 4 illustrates HOMO − 2 for **3**, which is one of the most striking; this is the fully bonding π-orbital and clearly shows twisted, p−p π-interactions of the appropriate phase. A pleasant feature of this analysis is that it permits a ready explanation of all of the differences in the spectra of **2** and **3** by considering the perturbing effect of the additional nitrogen atoms present in **2** but not in **3**. The three nonbonding lone pairs on the hydrazido β-nitrogen atoms also combine to give three symmetry-adapted hybrid orbitals, all of which are doubly occupied: in D_{3h} symmetry, there would be one hybrid belonging to the a_2'' irrep and two degenerate hybrids belonging to the e_x'' and e_y'' irreps. The energy separation between the three is very small because the nitrogen atoms are far from one another in space, but these orbitals can mix strongly with the TMM π-orbitals as indicated in Figure 3. The strongest interaction is between the sets of e-type orbitals as they are closest to one another in energy. As all of the e-type orbitals are doubly occupied, this has the effect of raising the energy of the HOMO and HOMO − 1 relative to the LUMO, which mixes much less efficiently with the remaining β-nitrogen hybrid. This rationalizes the lower energy of this absorption in **2** compared to **3**. Moreover, the mixing of the two sets of e-type orbitals creates a second degenerate level only somewhat below the first, and this rationalizes the HOMO − 3 and HOMO − 4 to LUMO excitations observed in **2** but not in **3** (there are such absorptions in **3**, of course, but the HOMO − 3 and HOMO − 4 orbitals will have entirely different character in that case).

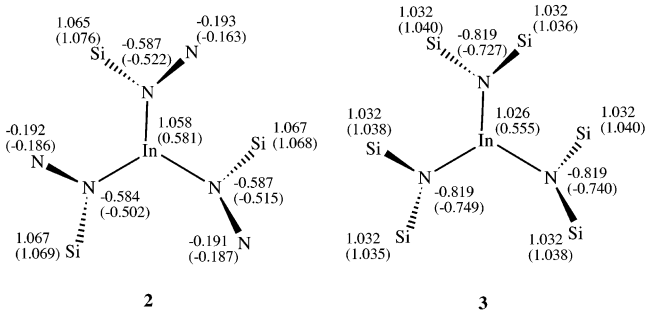

Figure 5. Calculated Mulliken charges at the CIS/STO-3G level for selected heavy atoms in the ground and first excited states of $In[N(SiMe_3)NMe_2]_3$ (**2**) and $In[N(SiMe_3)_2]_3$ (**3**). Values in parentheses are those for the first excited state. Methyl groups are omitted for clarity.

Refining these points, note that the very different electronegativities of In and N ensure that it is nitrogen p character that dominates the lower energy orbitals and indium p character that dominates the empty orbitals. The LUMO in both **2** and **3** is formed almost entirely from the indium p, and all of the transitions already discussed may thus be regarded as having substantial ligand-to-metal charge transfer character. Indeed, Mulliken charge distributions computed for the ground state at the HF/STO-3G level and for the first excited state at the CIS/STO-3G level are shown in Figure 5 and support the interpretation that the longest-wavelength excitation mainly involves ligand-to-metal charge transfer. For compound **2**, the positive charge on the indium decreases by 0.477 on going from the ground state to the first excited state, indicating a gain of electron density. The total negative charge on the three α-nitrogens decreases by 0.219, that on the β-nitrogens by 0.040, and the remaining ligand charge depletion is spread over the other atoms. Similar charge transfer transitions are observed for compounds **3** and **4**. Consistent with the LMCT nature of these transitions, the more electropositive nature of the $[N(SiMe_3)_2]$ ligand in **3** raises the energy of all absorptions relative to those observed in **4**, which has a *t*-Bu group substituted for one of the $SiMe_3$ substituents. While one might anticipate that the yellow to brown colors reported for $In(NPh_2)_3(py)$,[27] $In[NMe(SiMe_3)]_3$-(*p*-Me_2Npy),[27] $In[N(H)(2,6\text{-}^iPr_2C_6H_3)]_3(py)_2$,[31] and $In[N(H)$-$(2,4,6\text{-}^tBu_3C_6H_2)]_3$[31] are due to LMCT transitions, the change in coordination number for the first three complexes and the absence of any electronic absorption spectra preclude more detailed comparisons.

For the hydrazido gallium complex, **1**, analogous LMCT transitions would be expected to occur at lower energy with respect to **2**. Consistent with the colorless nature of both the crystals and solution of **1**, no absorptions were detected at wavelengths longer than 350 nm. The cause of the missing transitions may be the result of geometric changes in **1** due to the smaller metal. Sterically crowded ligands could force a more nearly perpendicular orientation relative to the GaN_3 plane. Even more substantial differences involving complexation of the hydrazido β-nitrogens are possible. As a result, the observed absorption at 295 nm cannot be assigned to a specific transition.

Last, the LUMO + 1 orbital is observed to be a fully symmetric combination of In−N σ*-orbitals. This explains

the dipole-allowedness of transitions from the π-system to this orbital that occur at substantially higher energies than the $\pi-\pi$ transitions.

Conclusions

Routine methods were used to synthesize the tris(hydrazides) of gallium and indium in good yields. Although analysis of the molecular structure of $In[N(TMS)NMe_2]_3$ does not provide evidence for In−N bond shortening that is associated with π-bonding, spectroscopic and theoretical studies verify its presence. The unexpected yellow color of the In compound resulted from mixing of the β-nitrogen lone pairs with the trimethylenemethane-like molecular orbitals of the InN_3 core. This mixing resulted in raising the HOMO and lowering the energy of the ligand-to-metal charge transfer responsible for the lowest energy transition.

Acknowledgment. The authors gratefully acknowledge support from the National Science Foundation (CHE-9616501 and CHE-0203346), thank Prof. Kent Mann and Mr. Daron Janzen for their assistance in the experiments for obtaining the absorption spectra, and thank Dr. Victor G. Young for his help with the single crystal XRD experiment.

Supporting Information Available: X-ray crystallographic file in CIF format for the structure determinations of compound **2**. This material is available free of charge via the Internet at http://pubs.acs.org.

IC020693F